# Road Maintenance Prioritization (RMP) System

İsmail Rakıp Karaş[1], Sohaib K. M. Abujayyab[2], Osama Afana[1], Mewloud Saghir[1]

[1] Department of Computer Engineering, Karabuk University, Demir Çelik Campus, 78050 Karabuk, Türkiye
ismail.karas@karabuk.edu.tr, osamaafana4@gmail.com , sgmewloud@gmail.com
[2]Department of Geography, Karabuk University, Demir Çelik Campus, 78050 Karabuk, Türkiye
sjayyab@karabuk.edu.tr

**Keywords:** GIS-Based Decision Support; Road Maintenance Prioritization; Analytic Hierarchy Process (AHP); Remote Sensing; Traffic Load Analysis

**Abstract**

This study develops a transparent, weighted framework for assessing road condition and prioritizing maintenance at the segment level. Traffic data (AADT/ESAL) are fused with climate and terrain layers extracted via Google Earth Engine (GEE) into a national spatial database. A Final Road Condition Index (FRCI; 0–100) is derived from eight weighted criteria (CTDI, slope, vegetation, surface water, topographic wetness, precipitation, snow, erosion), updated periodically to reflect changing conditions. The framework was applied to Türkiye's national road network managed by the General Directorate of Highways (KGM). Environmental rasters were sampled every 5 km along road centerlines, traffic was converted to ESAL and normalized to CTDI, and the FRCI was computed as a weighted sum. An interactive Streamlit dashboard with a MySQL/PostgreSQL backend enables visualization, sensitivity testing, and AI-driven treatment recommendations, benchmarked against KGM's current inspection-based system. Results show that incorporating GEE layers improved prioritization compared to AADT-only baselines, increased decision consistency, reduced time-to-decision, and yielded higher benefit under fixed budgets. The suggestion engine provided more consistent, better-justified recommendations. The study recommends adopting the FRCI framework nationally, institutionalizing periodic GEE updates, formal governance of weights and criteria, and embedding the dashboard and suggestion engine into KGM's annual planning cycle for more efficient, evidence-based maintenance.

## 1. Introduction

### 1.1 Background and Motivation

Türkiye's 68,000 km highway network links industrial hubs, ports, and rural communities. Pavement distress rutting, cracking, potholes intensifies where heavy traffic loads coincide with harsh climatic and topographic conditions. Agency practices centered on visual surveys and ad-hoc traffic counts capture only snapshots of a multifactor problem, often leading to reactive rather than preventive planning.

### 1.2 Problem Statement

KGM allocates maintenance funds largely from periodic visual inspections and annual traffic volumes. These inputs under-represent spatial/temporal variability (e.g., freeze thaw in the Black Sea, extreme heat on the Mediterranean, steep grades, drainage deficiencies) and can misallocate scarce budgets. We frame the challenge as a geospatial decision problem: segment the national network; enrich with multi-source layers traffic loading (ESAL/AADT), climate normals and extremes, terrain (slope/erosion), land-use context—within a unified spatial database; compute segment-level composite risk indicators; and expose explainable, cost-aware treatment suggestions at the point of decision.

**Gap.** There is no integrated, auditable workflow that continuously refreshes spatially granular risk indices at national scale, translates those risks into transparent, cost-aware treatments with expected benefits, and consistently grounds decisions in up-to-date standards and historical contracts. This necessitates a GIS-centric, AIassisted framework that fuses heterogeneous data to generate explainable, segment-level recommendations tied to verifiable documentary evidence.

### 1.3 Main Research Question

How can a weighted framework with systematically assigned feature weights provide an integrated, auditable workflow that continuously updates segment-level risk indices (FRCI), translates them into transparent and cost-effective maintenance treatments, and grounds each recommendation in current agency standards and historical records?

### 1.4 Sub-questions

1. To what extent does using GEE to derive risk indices from traffic, climate, and terrain improve maintenance prioritization compared with current KGM practices?
2. How can AI-driven maintenance suggestion engines enhance decision consistency and cost-effectiveness compared with purely rule-based or ad-hoc approaches?

### 1.5 Research Objectives

1. **Data Fusion:** Integrate historical KGM traffic datasets with GEE environmental layers in a unified spatial database.
2. **Composite Metric:** Develop a scalable FRCI by systematically assigning weights to traffic and environmental features to quantify segment-level risk on a 0–100 scale.
3. **Decision Support:** Build an SQL-backed dashboard plus an AI-driven suggestion engine for consistent, transparent recommendations aligned with institutional standards and records.


https://doi.org/10.5194/isprs-archives-XLVIII-4-W18-2025-173-2026  

## 2. Literature Review & Previous

### 2.1 Highway Maintenance Prioritisation Paradigms

Early approaches relied on the Pavement Condition Index (PCI) (Shahin, 2005). Deterministic models used deterioration curves vs. cumulative ESALs (Paterson, 1987). Recent work leverages ML on sensor imagery (Gopalakrishnan, 2018).

| Era | Primary Data | Method | Limitation |
|---|---|---|---|
| 1980s | Visual PCI | Manual ranking | Subjective |
| 1990s | PCI + AADT | HDM-III models | Static curves |
| 2010s | LIDAR, GPR | ML classifiers | Data-hungry |
| 2020s | Multisource fused | Deep ensembles | Explainability |

Table 1. Comparison of highway-maintenance prioritisation methods

### 2.2 Environmental Factors in Road Deterioration

Thermal cracking accelerates with high diurnal temperature swings; freeze–thaw cycles induce potholes via icelens expansion (Qiu et al., 2022). Vegetation indices (NDVI) relate to moisture retention and subgrade condition (U.S. Geological Survey, 2011).

### 2.3 Traffic-Load Impact Assessment

ESAL normalizes mixed traffic; heavy vehicles dominate fatigue damage (∝ axle load4) (Huang, 2004). Speed regimes matter: high-speed corridors vs. stop-and-go (Gillespie et al., 1993).

### 2.4 Multi-Criteria Decision Analysis in Infrastructure

AHP is widely adopted for transparency (Saaty, 1980). Fuzzy AHP and TOPSIS handle uncertainty (Kahraman et al., 2004; Hwang and Yoon, 1981). GIS–MCDA frameworks exist for related risks (Malczewski, 2006).

### 2.5 Representative Prior Studies

**Remote sensing for roadway condition.** Comprehensive review linking remote sensing to road evaluation (Schnebele et al., 2015).
**Automated inspection at scale.** Smartphone imagery with deep neural networks for road damage detection (Maeda et al., 2018).

## 3. Methodology

### 3.1 Study Population

All segments of Türkiye’s national KGM network (expressways, primary, secondary). Each segment has a KKNO identifier.

### 3.2 Study Sample

Segments in the database after ETL:

- point sampling ~5 km along each segment from environmental/terrain rasters;
- aggregation to KKNO level for index construction and analyses.

### 3.3 Data Sources

| Data | Satellite / Product | Feature(s) / Notes |
|---|---|---|
| Traffic (KGM, 2024) | KGM (official counts) | AADT at dilim per KKNO; transformed to ESAL. |
| GEE rasters | *Sentinel-2 MSI Landsat-8 L2* | NDVI, NDWI Land Surface Temperature (LST) |
| | *CHIRPS* | Precipitation |
| | *SRTM* | Elevation, Slope, Roughness |
| | *HydroSHEDS* | Flow → TWI |
| | *MODIS* | Snow cover |
| | *Sentinel-5P* | Aerosols / dust |
| | *VIIRS DNB* | Night lights |
| | *SMAP* | Soil moisture |
| Derived | — | Erosion Risk = Slope × Precipitation. |
| Time window | — | 2022-01-01 to 2024-12-31; harmonized at 100 m scale. |

Table 2. Core data sources and processing summary.

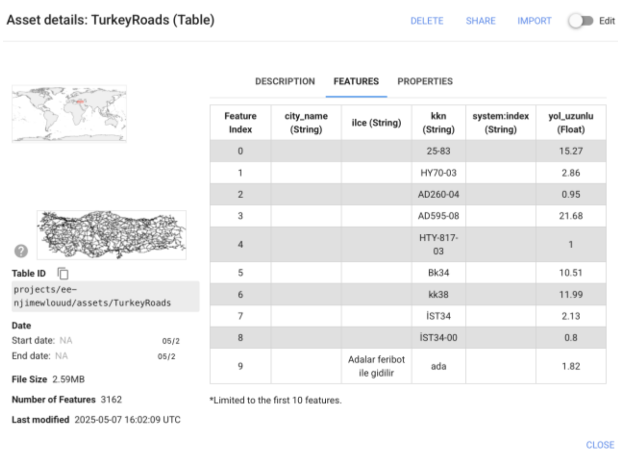


Figure 1. Study frame: national KGM network.

### 3.4 GEE Pipeline and Sampling

The area is tiled for processing; centerlines are densified with samples every ~5 km. Time-averaged composites are made per raster (2022–2024), then values are extracted with sampleRegions (scale 100 m) and exported to CSV.

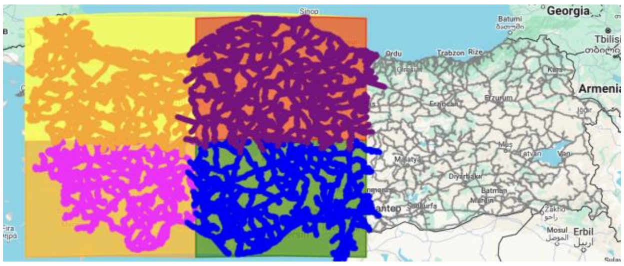


Figure 2. Collecting rasters from Google Earth Engine.

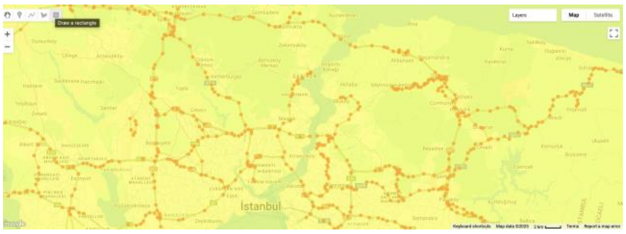


Figure 3. Sampling scheme along road centerlines (∼5 km spacing).

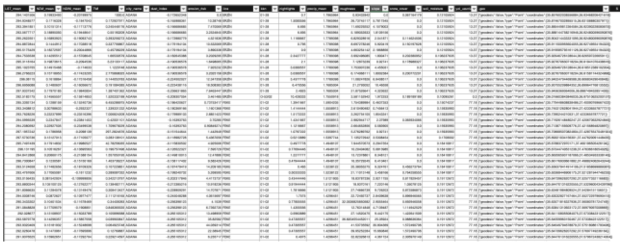

Figure 4. Example of extracted climate/terrain variables.

### 3.5 Traffic Data Processing (ETL 2024)

The 2024 workbook (all sheets) is loaded; two-row headers are flattened and standardized; a year=24 tag is added; numeric types are coerced. Key fields: BL.NO, İLİ, KKNO, DİLİM NO, UZUNLUK KM, SAYIM TÜRÜ, and traffic volumes (YOGT) by class (car/medium truck/bus/truck/truck+trailer). ESAL factors: car 0.0004, medium truck 0.5, bus 0.7, heavy truck 1.5, truck+trailer 2.0.

$$\text{Daily\_ESAL} = \sum\nolimits_c \left(\text{vehicle\_count}_c \times \text{ESAL\_factor}_c\right) \tag{1}$$

$$\text{CTDI\_ESAL\_km} = \frac{\text{Daily\_ESAL}}{\text{UZUNLUK\_KM}} \tag{2}$$

CTDI is robust-scaled by trimming the 1–99% quantiles and applying min–max to 0–100 to yield CTDI_norm; CTDI_status buckets are built with bins [−1, 5, 12, 100] labeled low/normal/high. Dilim rows are collapsed to the KKNO level by summing volumes/length/ESAL, averaging speed/violation metrics, computing length-weighted CTDI_ESAL_km and CTDI_norm, and selecting the worst CTDI_status when multiple exist. Outputs are saved to CSV and to database tables: **traffic_data, traffic_output, google_earth_engine_data, and final_result.**

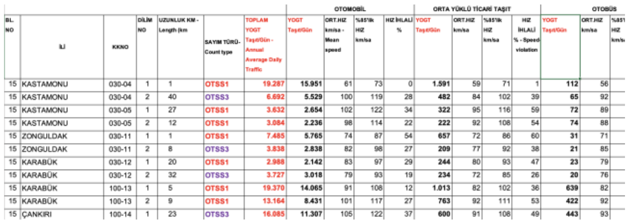

| | | | | | | | OTOMOBİL | | | | ORTA YÜKLÜ TİCARİ TAŞIT | | | | OTOBÜS | | |
|---|---|---|---|---|---|---|---|---|---|---|---|---|---|---|---|---|---|
| BL. NO | İLİ | KKNO | DİLİM NO | UZUNLUK KM - Length (km | SAYIM TÜRÜ- Count type | TOPLAM YOGT Taşıt/Gün - Annual Average Daily Traffic | YOGT Taşıt/Gün | ORT.HIZ km/sa - Mean speed | %85'lik HIZ km/sa | HIZ İHLALİ % | YOGT Taşıt/Gün | ORT.HIZ km/sa | %85'lik HIZ km/sa | HIZ İHLALİ % - Speed violation | YOGT Taşıt/Gün | ORT.HIZ km/sa | %85'l HIZ km/s |
| 15 | KASTAMONU | 030-04 | 1 | 1 | OTSS1 | 19.287 | 15.951 | 61 | 73 | 0 | 1.591 | 59 | 71 | 1 | 112 | 56 | |
| 15 | KASTAMONU | 030-04 | 2 | 40 | OTSS3 | 6.692 | 5.529 | 100 | 119 | 28 | 482 | 84 | 102 | 39 | 65 | 92 | |
| 15 | KASTAMONU | 030-05 | 1 | 27 | OTSS1 | 3.632 | 2.654 | 102 | 122 | 34 | 322 | 95 | 116 | 59 | 72 | 89 | |
| 15 | KASTAMONU | 030-05 | 2 | 12 | OTSS1 | 3.084 | 2.236 | 98 | 114 | 22 | 222 | 92 | 108 | 54 | 74 | 88 | |
| 15 | ZONGULDAK | 030-11 | 1 | 1 | OTSS1 | 7.485 | 5.765 | 74 | 87 | 54 | 657 | 72 | 86 | 60 | 31 | 71 | |
| 15 | ZONGULDAK | 030-11 | 2 | 8 | OTSS3 | 3.838 | 2.838 | 82 | 98 | 27 | 209 | 77 | 92 | 38 | 21 | 85 | |
| 15 | KARABÜK | 030-12 | 1 | 20 | OTSS1 | 2.988 | 2.142 | 83 | 97 | 29 | 244 | 80 | 93 | 47 | 23 | 79 | |
| 15 | KARABÜK | 030-12 | 2 | 32 | OTSS3 | 3.727 | 3.018 | 79 | 93 | 19 | 234 | 72 | 85 | 26 | 20 | 76 | |
| 15 | KARABÜK | 100-13 | 1 | 5 | OTSS1 | 19.370 | 14.065 | 91 | 108 | 12 | 1.013 | 82 | 102 | 36 | 639 | 82 | |
| 15 | KARABÜK | 100-13 | 2 | 9 | OTSS1 | 13.164 | 8.431 | 101 | 117 | 27 | 763 | 92 | 111 | 53 | 422 | 92 | |
| 15 | ÇANKIRI | 100-14 | 1 | 23 | OTSS3 | 16.085 | 11.307 | 105 | 122 | 37 | 600 | 91 | 108 | 49 | 443 | 93 | |

Figure 5. Traffic ETL snapshot and CTDI fields.

### 3.6 Final Road Condition Index (FRCI)

Criteria and weights (sum = 1.0): CTDI_norm 0.08, Slope 0.18, NDVI_mean 0.12, NDWI_mean 0.15, TWI 0.15, Precip_mean 0.10, Snow cover 0.12, Erosion risk 0.10. "Worse when higher": CTDI, Slope, TWI, Precip, Snow, Erosion. "Better when higher": NDVI, NDWI; these are inverted after normalization to $1 - \tilde{x}$ for semantic consistency. Normalization rescales to [0, 1] (log transforms for right-skewed variables as needed).

$$\mathrm{FRCI}_{\mathrm{raw}}(s) = \sum w_i\,\tilde{x}_i(s), \qquad \mathrm{FRCI}_{0\text{–}100} = \frac{\mathrm{raw} - \min}{\max - \min} \times 100. \tag{3}$$

Classification: Very Good ≤ 20; Good 20–40; Fair 40–60; Poor 60–80; Very Poor > 80. Traffic override rule: if CTDI_norm exceeds a high operational threshold, degrade one level.

### 3.7 Maintenance Suggestion Module

**Overview.** This module converts analytics (FRCI and constituent features) into short, consistent maintenance suggestions per segment. It runs a local Qwen model (Ollama qwen3:1.7b) as a controlled text generator: it never invents facts and only verbalizes provided fields and rule outcomes.

**Triggering.** Whenever a user clicks a point/segment on the map, the frontend resolves the KKNO and sends the payload.

**Inputs per segment.** FRCI (0–100) and class; CTDI_norm, Slope, Precip_mean, Snow cover, TWI, NDVI_mean/NDWI_mean, Erosion risk; rule-selected candidate treatments (e.g., crack sealing, patching, thin overlay, mill & overlay, drainage, slope stabilization, shoulder/ditch works) with costs and expected life extension.

**Generation policy.** Allowed: a concise recommendation, 2–3 driver bullets naming top factors, and an optional budget note (benefit-per-cost under a user budget). Forbidden: new numbers/thresholds, external/vendor knowledge, or re-ranking (ranking is done by the rule engine). Missing fields are called out briefly and default to a qualitative suggestion.

**Prompt & decoding.** System role: "Civil-infrastructure editor. Use only provided fields. Do not invent facts. Preserve numbers/units. Be concise." Selectable style (UI): academic-concise vs. operator-plain; language mirrors user locale (TR/EN). Temperature/top-p: 0.5/0.9 (or 0.2 for repeatable text). Max tokens: 256–512 (pop-ups), up to 1024 for printable summaries. Stateless calls (no cross-segment memory).

**Integration with the dashboard.** Map click → resolve KKNO → assemble payload (signals, candidates, costs/benefits, context flags) → call Qwen → render recommendation + drivers (+ budget note). Exports include the same text.

**Configuration summary.** Model: qwen3:1.7b (local); role: controlled NL rendering of rule outputs. Inputs: FRCI/class; CTDI_norm; Slope; Precip_mean; TWI; NDVI_mean/NDWI_mean; Snow; Erosion; length; unit cost; life extension; benefit-per-cost; context flags. Outputs: concise recommendation + driver bullets + optional budget line.

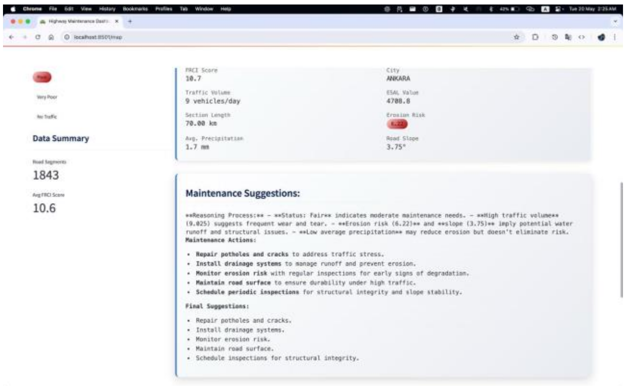


Figure 6. Segment-level suggestion panel after clicking a point on the map.

### 3.8 Document Assistant (RAG)

The document assistant provides auditable, just-in-time answers to engineering and policy questions by restricting generation to a curated corpus (standards, contracts, manuals, reports). It implements a classic retrieval-augmented generation loop with persistent vector indexing, conversational memory, and filename-level source display.

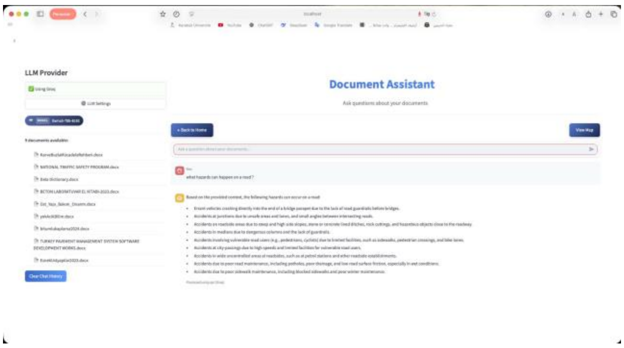


Figure 7. RAG assistant UI with sources.

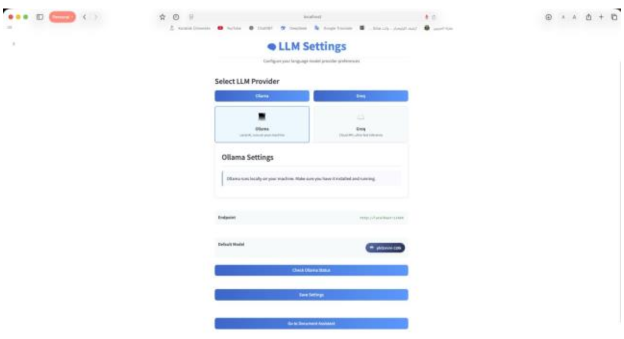


Figure 8. Local (Ollama) LLM settings.

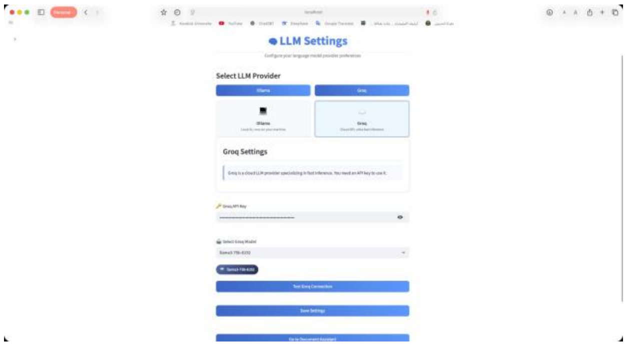


Figure 9. Optional Groq LLM settings.

## 4. Results and Analysis

### 4.1 Composite Traffic Density Index (CTDI)

Across 25,777 segments, 18 fall in the High-stress category, concentrated along the Istanbul–Ankara corridor and the Thrace freight belt.

### 4.2 Interactive National Map

The interactive FRCI overlay (Streamlit+Mapbox) supports filtering by status or city.

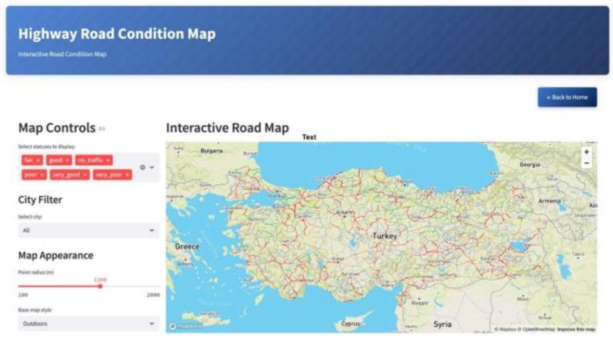


Figure 10. National FRCI map dashboard.

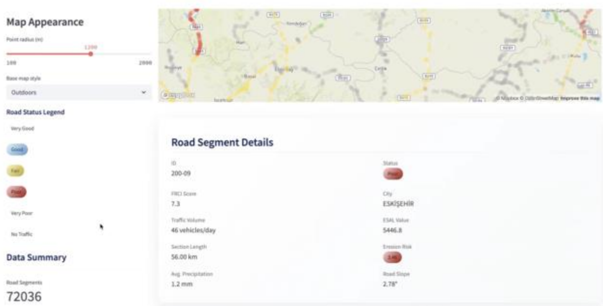


Figure 11. Point details panel in the interactive map.

### 4.3 Environmental Factor Analysis

Slope and precipitation are the strongest positive correlates with FRCI (worse condition).

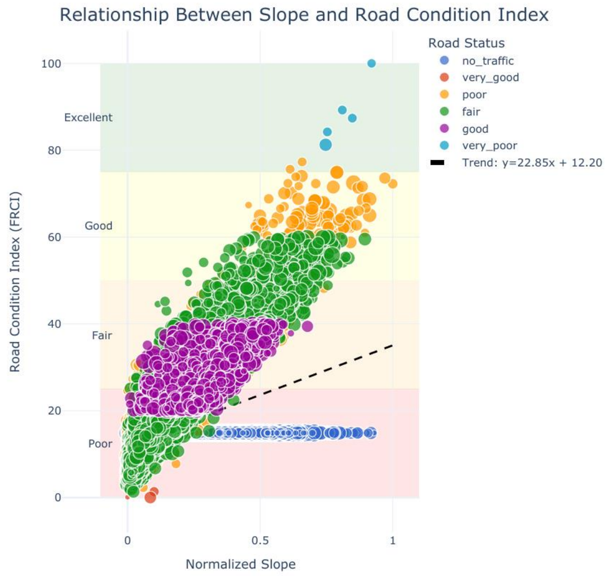


Figure 12. Association between slope and FRCI.

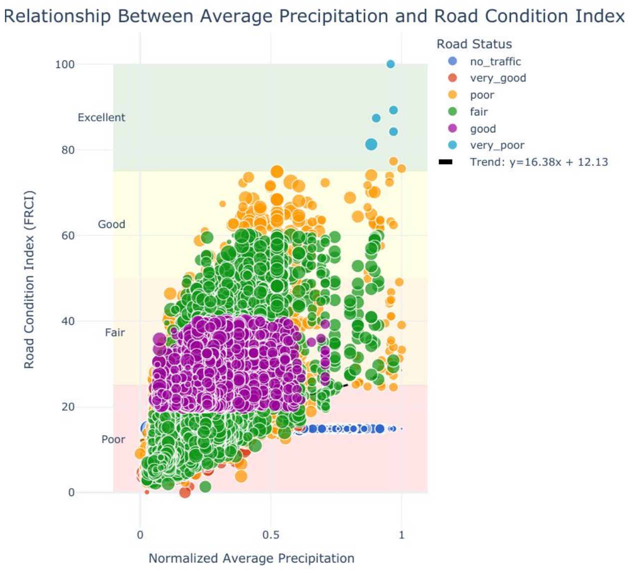


Figure 13. Association between precipitation and FRCI.

## 4.4 FRCI Analysis

Slope and precipitation are the strongest positive correlates with FRCI (worse condition).

**4.4.1 Distribution of Scores** Heavy left skew: 64% of segments have FRCI < 5 (no-traffic or very short links); the tail extends to > 60 in high-risk mountain passes.

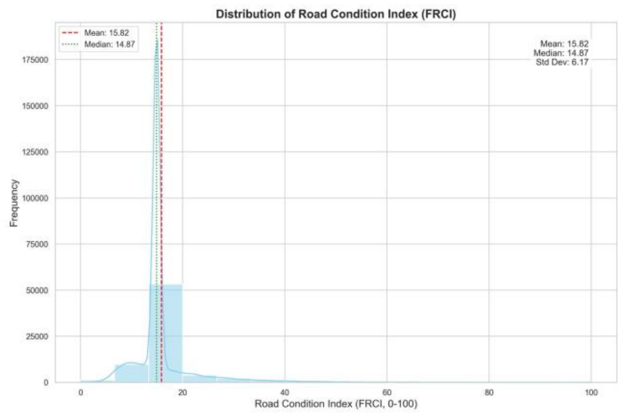


Figure 14. Distribution of the Road Condition Index (FRCI)

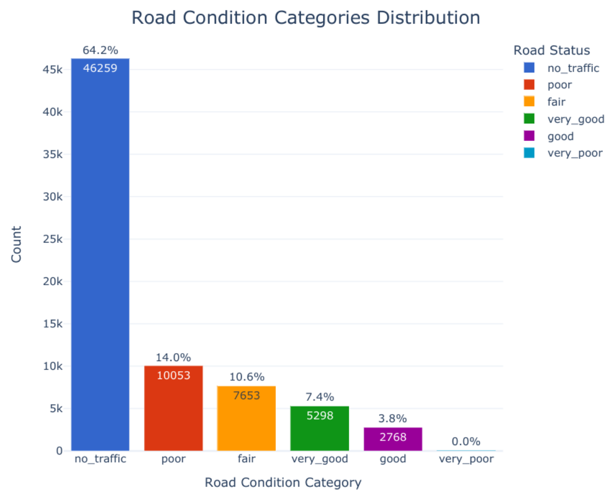


Figure 15. FRCI class breakdown across the network.

### 4.4.2 Category Breakdown

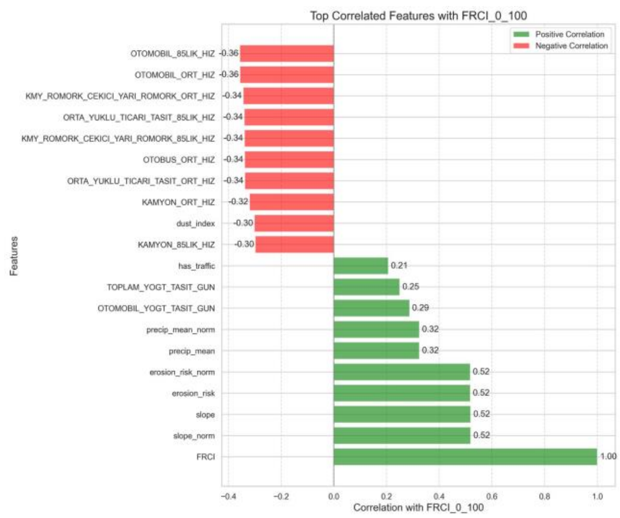


Figure 16. Top correlated features with FRCI (0–100).

### 4.5 Interactive Dashboard Highlights

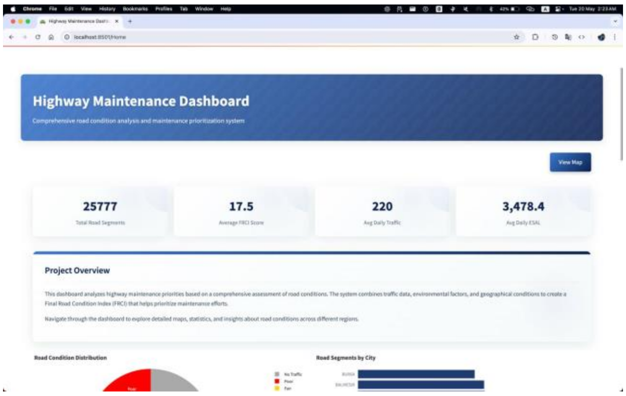


Figure 17. Dashboard main page overview.

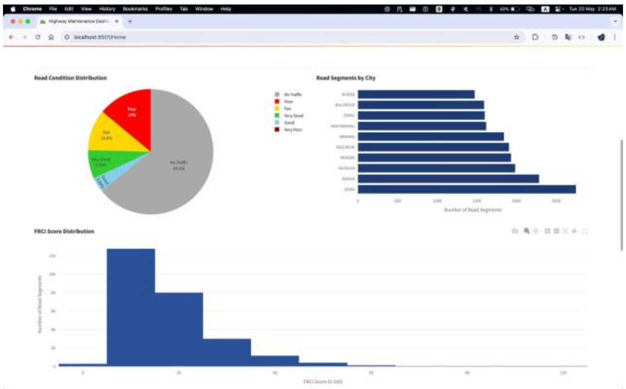


Figure 18. Key charts provided in the dashboard.

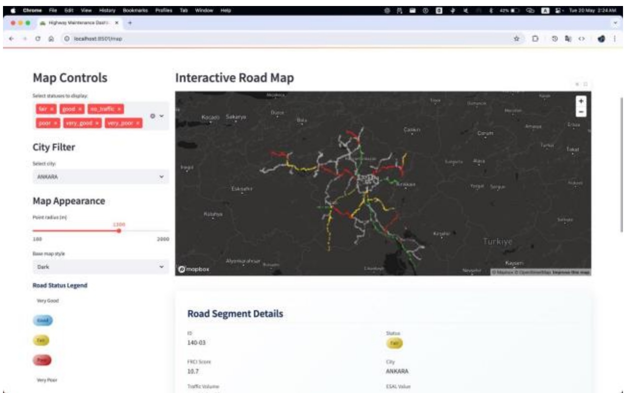


Figure 19. Filtering by city in the dashboard.

### 4.6 Case Study: Ankara Ring Road

Filtering to ANKARA yields 1,843 segments (Avg FRCI ≈ 10.6); the worst 5% align with steep grades (> 6%) and high ESAL.

### 4.7 Summary of Key Findings

- Traffic explains ~55% of FRCI variance; environmental factors ~45%.
- Slope and precipitation are the top environmental stressors.
- Re-allocating 20% of resurfacing budget to "Very Poor" segments would cut network-wide risk lane kilometres by ~35%.

## Acknowledgements

This study was supported by the Scientific and Technological Research Council of Türkiye (TÜBİTAK) under Grant Number 124N109. The authors thank TÜBİTAK for their support. We also thank collaborating agencies and colleagues for data access and feedback.

## References

Gillespie, T. D. et al., 1993. Effects of heavy-vehicle characteristics on pavement response and performance. Technical Report NCHRP Report 353, Transportation Research Board.

Gopalakrishnan, K., 2018. Deep Learning in Data-Driven Pavement Image Analysis and Distress Detection—A Review. Data, 3(3), 28. https://www.mdpi.com/2306-5729/3/3/28.

Huang, Y. H., 2004. Pavement Analysis and Design. 2edn, Pearson Prentice Hall, Upper Saddle River, NJ.
Hwang, C.-L., Yoon, K., 1981. Multiple Attribute Decision Making: Methods and Applications. Springer, Berlin.

Kahraman, C., Cebeci, U., Ruan, D., 2004. Multiattribute supplier selection using fuzzy AHP. International Journal of Production Economics, 97(2), 371–389. https://doi.org/10.1016/j.ijpe.2004.02.003.

Maeda, H., Sekimoto, Y., Seto, T., Kashiyama, T., Omata, H., 2018. Road damage detection and classification using deep neural networks with smartphone images. PLOS ONE, 13(3), e0206157. https://doi.org/10.1371/journal.pone.0206157.

Malczewski, J., 2006. GIS-based multicriteria decision analysis: a survey of the literature. International Journal of Geographical Information Science, 20(7), 703–726. https://doi.org/10.1080/13658810600661508.

Paterson, W. D. O., 1987. Road Deterioration and Maintenance Effects: Models for Planning and Management. The World Bank, Washington, DC.

Qiu, X., Meng, F., Li, Y., Chen, Z., Xu, W., 2022. Effects of Freeze–Thaw Cycles on Internal Voids and Voids Distribution of Asphalt Mixture. Materials, 15(11), 4003. https://www.mdpi.com/1996-1944/15/11/4003.

Saaty, T. L., 1980. The Analytic Hierarchy Process. McGraw–Hill, New York.

Schnebele, E., Tanyu, B., Cervone, G., Waters, N., 2015. Review of remote sensing methodologies for pavement management and assessment.EURO Journal on Transportation and Logistics / European Transport Research Review, 7, 18. https://etrr.springeropen.com/articles/10.1007/s12544-015-0156-6.

Shahin, M. Y., 2005. Pavement Management for Airports, Roads, and Parking Lots. 2 edn, Springer, New York.

U.S. Geological Survey, 2011. Ndvi and ndwi response to soil moisture in the san joaquin valley. Open-File Report 2011-1127, U.S. Geological Survey.